



# Journal of Applied and Computational Mechanics



Research Paper

## Nonlinear Vibration of an Electrostatically Actuated Functionally Graded Microbeam under Longitudinal Magnetic Field

Dang Van Hieu<sup>✉</sup>, Nguyen Thi Hoa<sup>✉</sup>, Le Quang Duy<sup>✉</sup>, Nguyen Thi Kim Thoa<sup>✉</sup>

TNU, Thai Nguyen University of Technology (TNUT), Thainguyn, Vietnam, Email: hieudv@tnut.edu.vn

Received October 22 2020; Revised February 17 2021; Accepted for publication February 17 2021.

Corresponding author: Dang Van Hieu (hieudv@tnut.edu.vn)

© 2021 Published by Shahid Chamran University of Ahvaz

**Abstract.** In this work, we develop a model of an electrostatically actuated functionally graded (FG) microbeam under a longitudinal magnetic field based on the Euler-Bernoulli beam and nonlocal strain gradient theories to investigate the nonlinear vibration problem. The FG microbeam is placed between two electrodes, a DC voltage applied between the two fixed electrodes causes an electrostatic force to be exerted on the FG microbeam. The FG microbeam is composed of metal and ceramic in which the properties of these materials are assumed to change in the thickness direction according to the simple power-law distribution. The Galerkin method and the Hamiltonian Approach are employed to find the approximate frequency of the FG microbeam. The accuracy of the present solution is verified by comparing the obtained results with the numerical results and the published results in the literature. Effects of the power-law index, the material length scale parameter, the nonlocal parameter, the applied voltage and the magnetic force on the nonlinear vibration behaviour of the FG microbeam are studied and discussed.

**Keywords:** Nonlinear vibration; Electrostatically actuated; Functionally graded microbeam; Longitudinal magnetic.

### 1. Introduction

Micro-/nano-structures have a wide range of applications in fields of engineering such as computer engineering, electrical-electronics engineering, automotive engineering, aerospace engineering, biomedical engineering, engineering optics, and so on [1 - 3]. In models of the micro-/nano-electromechanical systems (MEMS/NEMS), besides the fixed electrodes, the movable components are often modeled as micro-/nano-beams or micro-/nano-plates. The applied voltage causes an electrostatic force to act on the micro-/nano-beams or micro-/nano-plates, making them to vibrate. When the applied voltage is large, the micro-/nano-beams or micro-/nano-plates suddenly collapse toward the fixed electrodes, then the unstable phenomenon occurs. The unstable phenomenon in MEMS/NEMS models is called the pull-in instability [3]. The vibration and pull-in instability analyses of MEMS/NEMS models attract the attention of many scientists. The vibration response of clamped-clamped (C-C) microbeams subjected to an electric field was investigated by Batra et al. [4]. Rahman et al. [5] studied the nonlinear vibration behaviour of an electrically actuated Euler-Bernoulli microbeam considering effect of the midplane stretching. The nonlinear vibration of microbeams actuated by suddenly electrostatic force was investigated by Zand et al. [6] using the Homotopy analysis method. The nonlinear dynamic characteristics of electrostatically actuated microstructures under superharmonic excitations were reported by De and Aluru [7] employing numerical simulations. The dynamic pull-in instability of C-C microbeams subjected to a suddenly electrostatic force and nonlinear squeeze film damping was studied by Krylov [8] using the Lyapunov exponent criteria. The dynamic instability behaviour of curved shallow microbeams actuated by electrostatic forces was investigated by Krylov and Dick [9]. The dynamic behaviour of an imperfect microbeam subjected to electrostatic and electrodynamic actuations was investigated by Ruzziconi et al. [10] using the two single mode reduced-order model. The pull-in instability of electrostatically actuated micro-/nano-beams under Van der Waals force was reported by Askari and Tahani [11] using the homotopy perturbation method. The influences of the structural nonlinearity, air-gap thickness, electrode and plate lengths on pull-in instability phenomena of an electrostatically actuated cantilever microbeam attached a rigid microplate were investigated by Harsha et al. [12]. The analytical form of static pull-in voltage of C-C Euler-Bernoulli microbeams subjected to electrostatic loading and Casimir force was found by Bhojawala and Vakharia [13]. The onset of nonlinear dynamics was proposed by Hasan et al. [14] to activate a microbeam subjected to electrostatic actuation as a tunable-threshold pressure sensor. The static and dynamic behaviours of MEMS arches actuated by fringing-field electrostatic force were investigated by Ouakad [15], Tausiff et al. [16, 17] and Ouakad and Sedighi [18]. The nonlinear dynamic behaviours of MEMS resonators were studied by some authors [19-23]. Vibration analysis of another MEMS/NEMS model in which micro-/nano-beams are placed between the two fixed electrodes was also investigated by Fu et al. [24] using the energy balance method, Qian et al. [25] utilizing the homotopy analysis method, Hieu et al. [26] employing the equivalent linearization and the parameter expansion methods. The electric excitation caused by the voltage applying on the fixed electrodes drive the vibration of the micro-/nano-beams.

Based on an ideal is to make a composite material by varying the micro-/nano-structure from one material to another material with a specific gradient, the functionally graded materials (FGMs) have outstanding advantages compared to the traditional



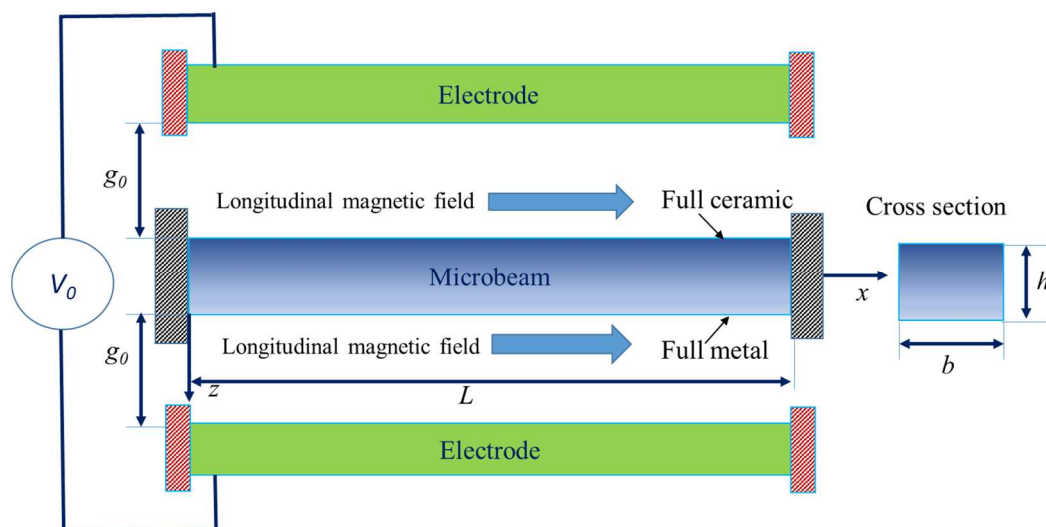
composite materials. FGMs are increasingly having many applications in different industrial fields such as nuclear reactor, aerospace, aircrafts, automobile and biomedical industries [27]. Research on the static and dynamic behaviours of FG structures has been of particular interest to scientists recently. Several works focusing on analysis of the static and dynamic characteristics of FG beams using various differential beam theories were reported such as the higher-order shear deformation beam theory [28 - 31] and the quasi-3D beam theory [32]. The bending, buckling and vibration behaviours of FG plates are also investigated by many authors using different plate theories including the shear deformation plate theory [33 - 35], the variable refined plate theory [36, 37] and the quasi-3D shear deformation plate theory [38, 39].

The size-dependent effects are very important for the mechanical behaviour of micro-/nano-structures. The classical continuum mechanics is not suitable for describing the mechanical behaviour of these structures because of the lack of length scale parameters. Some higher-order elasticity theories have been developed that can describe the size-dependent influences on the mechanical response of micro-/nano-structures such as the nonlocal elasticity theory (NET) [40, 41], the strain gradient theory (SGT) [42-44], the modified couple stress theory (MCST) [45]. And recently, in 2015, Lim et al. [46] combined the nonlocal elasticity and strain gradient theories in a generalized elasticity theory, this elasticity theory is called the nonlocal strain gradient theory (NSGT). In the NSGT, the size-dependent effect is observed through the nonlocal parameter and the material length scale parameter. The vibration and instability behaviours of MEMS/NEMS models were effectively studied by using these higher-order elasticity theories. Kivi et al. [47] investigated the nonlinear static and dynamic responses of a nanobeam subjected to an electrostatic actuation using the MCST. The size-dependent effect on pull-in characteristic of electrostatically actuated microbeams was investigated by Kong [48] employing the MCST. The static pull-in instability behaviour of NEMS considering the effect of Casimir force was investigated by Beni et al. [49] using the MCST and the Adomian decomposition. Based on the MCST and the Fredholm integral equation, the static pull-in behaviour of electrostatic microactuators was studied by Rokni et al. [50]. Employing the SGT, Sedighi [51] investigated the dynamic pull-in instability behaviour of electrically actuated microbeams. Effects of surface energy, Casimir and Van der Waals forces on the pull-in stability response of nanobridges were investigated by Sedighi [52] using the NET. The effects of intermolecular forces on the pull-in instability behaviour of an electrostatically actuated FG cantilever nanobeam were studied by Ataei and Beni [53] utilizing the SGT. Based on the NSGT, the nonlinear vibration of nanobeam subjected to the electrostatic force was investigated by Dang et al. [54] using the equivalent linearization method and the variation approach. And, Esfahani et al. [55] using the differential quadrature method and the NSGT to study the nonlinear vibration behaviour of an electrostatic FG nanoresonator considering the effect of the residual surface stress.

It can see that works related to analyze of the static and dynamical behaviours of electrostatically actuated FG micro-/nano-beams are very limited. The influence of the magnetic field on the nonlinear vibration response of electrostatically actuated FG micro-/nano-beams based on the NSGT has not been studied. In this work, the nonlinear vibration behaviour of an electrostatically actuated FG microbeams under magnetic field is presented for the first time in the framework of the NSGT and the Euler-Bernoulli beam theory (EBT). The vibration of the FG microbeam is dominated by an electrostatic force caused by the DC voltage applied between the two electrodes. The analytical expression of the approximate nonlinear frequency of the FG microbeam is obtained via the Galerkin method and the Hamiltonian Approach. Comparing the obtained results with the numerical and published results proves the accuracy of the current solution. Numerical studies are carried out to examine influences of the parameters on the nonlinear vibration behaviour of the FG microbeam.

## 2. Modelling and Equations

A 2D model of an electrostatically actuated FG microbeam under a longitudinal magnetic field is considered as in Fig. 1. This model was first proposed by Fu et al. [24] to study the nonlinear vibration behaviour of the microbeam via the Energy Balance method, and this model is further studied by some authors [25, 26, 55]. The microbeam with two clamped ends is assumed to be composed of two materials including ceramic ("c") and metal ("m"). The FG microbeam has a length  $L$  and a cross-sectional area  $b \times h$ . The FG microbeam is placed between two fixed electrodes. A DC current with voltage  $V_0$  applied between the two fixed electrodes exerts an electrostatic force on the FG microbeam. Initial gap from the FG microbeam to the two fixed electrodes is  $g_0$ . Besides the influence of the electrostatic force, the FG microbeam are also considered to be subjected to a longitudinal magnetic field. The coordinate system is considered in Fig. 1 in which  $x$  and  $z$  are the coordinates along the length and thickness directions of the FG microbeam, respectively.



**Fig. 1.** 2D modelling of an electrostatically actuated FG microbeam under longitudinal magnetic field



The material property of the microbeam varies as a function of the thickness coordinate ( $z$ ). Based on the simple power-law distribution, the Young's modulus  $E(z)$  and the material density  $\rho(z)$  are expressed as [56, 58, 59]:

$$E(z) = (E_c - E_m) \left( \frac{z}{h} + \frac{1}{2} \right)^k + E_m \quad (1)$$

$$\rho(z) = (\rho_c - \rho_m) \left( \frac{z}{h} + \frac{1}{2} \right)^k + \rho_m \quad (2)$$

where  $k$  is the power-law index governing the distribution of materials that make up the microbeam;  $E_c$  and  $\rho_c$  denote the Young's modulus and the material density of ceramic, respectively; and  $E_m$  and  $\rho_m$  denote respectively the Young's modulus and the material density of metal. It shows that  $E = E_c$  as  $k = 0$ , it means that the microbeam is composed of full ceramic. On the other hand, when  $k \rightarrow \infty$ ,  $E = E_m$  that is the microbeam is composed of full metal. As can be observed from Eqs. (1) and (2) that  $E = E_m$  as  $z = -h/2$  and  $E = E_c$  as  $z = h/2$ ; it means that the bottom surface of the FG microbeam is rich in metal while the top surface of the FG microbeam is rich in ceramic.

In this work, the EBT and the NSGT [46] are utilized to derive the equation of motion for the FG microbeam. Accordingly, the equation of motion for the FG microbeam is given by [58]:

$$D_{xx} \left( 1 - I_m^2 \frac{\partial^2}{\partial x^2} \right) \frac{\partial^4 w}{\partial x^4} + \left\{ -\frac{A_{xx}}{2L} \int_0^L \left( \frac{\partial w}{\partial x} \right)^2 dx + \frac{A_{xx}}{L} I_m^2 \int_0^L \left[ \frac{\partial w}{\partial x} \frac{\partial^3 w}{\partial x^3} + \left( \frac{\partial^2 w}{\partial x^2} \right)^2 \right] dx \right\} \left[ \frac{\partial^2 w}{\partial x^2} - (ea)^2 \frac{\partial^4 w}{\partial x^4} \right] + m_0 \frac{\partial^2}{\partial t^2} \left[ w - (ea)^2 \frac{\partial^2 w}{\partial x^2} \right] = \left[ q - (ea)^2 \frac{\partial^2 q}{\partial x^2} \right]. \quad (3)$$

where  $D_{xx}$ ,  $A_{xx}$  and  $m_0$  are the bending coefficient, the extensional coefficient and the mass moments of inertia of the FG microbeam, respectively, which are defined as follows:

$$D_{xx} = \int_A E(z) z^2 dA = b \int_{-h/2}^{h/2} \left[ (E_c - E_m) \left( \frac{z}{h} + \frac{1}{2} \right)^k + E_m \right] z^2 dz \quad (4)$$

$$A_{xx} = \int_A E(z) dA = b \int_{-h/2}^{h/2} \left[ (E_c - E_m) \left( \frac{z}{h} + \frac{1}{2} \right)^k + E_m \right] dz \quad (5)$$

$$m_0 = \int_A \rho(z) dA = b \int_{-h/2}^{h/2} \left[ (\rho_c - \rho_m) \left( \frac{z}{h} + \frac{1}{2} \right)^k + \rho_m \right] dz \quad (6)$$

In the right hand side of Eq. (3),  $q = q_e + q_m$  is the transverse distribution force consisting of the electrostatic force ( $q_e$ ) and the magnetic force ( $q_m$ ). The electrostatic force  $q_e$  is the driving force per unit length of the FG microbeam which results from electrostatic excitation [24-26, 55]:

$$q_e = \frac{\epsilon_v b V_0^2}{2} \left[ \frac{1}{(g_0 - w)^2} - \frac{1}{(g_0 + w)^2} \right], \quad (7)$$

where  $\epsilon_v \approx 8.85 \times 10^{-12} \text{ F/m}$  is the dielectric constant. In this work, a steady axial magnetic field is considered, the magnetic force per unit length of the FG microbeam is the Lorentz force [57]:

$$q_m = \eta A H_x^2 \frac{\partial^2 w}{\partial x^2}, \quad (8)$$

in which,  $\eta$  is the magnetic permeability and  $H_x$  is the component of the longitudinal magnetic field vector exerted on the FG microbeam in the  $x$ -direction.

Equation (3) is the nonlinear partial differential equation (PDE); with two clamped ends, kinematic boundary conditions of the FG microbeam are described as follows:

$$w(0, t) = w(L, t) = \frac{\partial w(0, t)}{\partial x} = \frac{\partial w(L, t)}{\partial x} = 0 \quad (9)$$

For convenience, the following dimensionless variables are defined:

$$\bar{x} = \frac{x}{L}, \bar{w} = \frac{w}{L}, \bar{t} = t \sqrt{\frac{E_m h^2}{\rho_m L^4}}, \alpha = \frac{l_m}{L}, \beta = \frac{ea}{L}, \delta = \frac{g_0}{h}, V = \sqrt{\frac{24 \epsilon_v V_0^2 L^4}{E_m g_0^3 h^3}}, H = \sqrt{\frac{\eta A H_x^2 L^2}{E_m b h^3}}, \bar{z} = \frac{z}{h}. \quad (10)$$

Using Eq. (10), the equation of motion for the FG microbeam is rewritten in the following dimensionless form:

$$\begin{aligned} & \bar{D}_{xx} \left( \frac{\partial^4 \bar{w}}{\partial \bar{x}^4} - \alpha^2 \frac{\partial^6 \bar{w}}{\partial \bar{x}^6} \right) + \left\{ -\frac{\bar{A}_{xx}}{2} \delta^2 \int_0^1 \left( \frac{\partial \bar{w}}{\partial \bar{x}} \right)^2 d\bar{x} + \bar{A}_{xx} \alpha^2 \delta^2 \int_0^1 \left[ \frac{\partial \bar{w}}{\partial \bar{x}} \frac{\partial^3 \bar{w}}{\partial \bar{x}^3} + \left( \frac{\partial^2 \bar{w}}{\partial \bar{x}^2} \right)^2 \right] d\bar{x} \right\} \left[ \frac{\partial^2 \bar{w}}{\partial \bar{x}^2} - \beta^2 \frac{\partial^4 \bar{w}}{\partial \bar{x}^4} \right] + \bar{m}_0 \left[ \frac{\partial^2 \bar{w}}{\partial \bar{t}^2} - \beta^2 \frac{\partial^4 \bar{w}}{\partial \bar{t}^2 \partial \bar{x}^2} \right] \\ & - H^2 \left[ \frac{\partial^2 \bar{w}}{\partial \bar{x}^2} - \beta^2 \frac{\partial^4 \bar{w}}{\partial \bar{x}^4} \right] - \frac{V^2}{48} \left[ \frac{1}{(1 - \bar{w})^2} - \frac{1}{(1 + \bar{w})^2} \right] + \frac{V^2 \beta^2}{8} \left[ \frac{1}{(1 - \bar{w})^4} - \frac{1}{(1 + \bar{w})^4} \right] \left( \frac{\partial \bar{w}}{\partial \bar{x}} \right)^2 + \frac{V^2 \beta^2}{24} \left[ \frac{1}{(1 - \bar{w})^3} + \frac{1}{(1 + \bar{w})^3} \right] \frac{\partial^2 \bar{w}}{\partial \bar{x}^2} = 0. \end{aligned} \quad (11)$$

where



$$\bar{D}_{xx} = \int_A \frac{E(z)z^2}{E_m} dA = bh^3 \int_{-1/2}^{1/2} \left[ \left( \frac{E_c}{E_m} - 1 \right) \left( \bar{z} + \frac{1}{2} \right)^k + 1 \right] \bar{z}^2 d\bar{z} \quad (12)$$

$$\bar{A}_{xx} = \int_A \frac{E(z)}{E_m} dA = bh \int_{-1/2}^{1/2} \left[ \left( \frac{E_c}{E_m} - 1 \right) \left( \bar{z} + \frac{1}{2} \right)^k + 1 \right] d\bar{z} \quad (13)$$

$$\bar{m}_0 = \int_A \frac{\rho(z)}{\rho_m} dA = bh \int_{-1/2}^{1/2} \left[ \left( \frac{\rho_c}{\rho_m} - 1 \right) \left( \bar{z} + \frac{1}{2} \right)^k + 1 \right] d\bar{z} \quad (14)$$

The kinematic boundary conditions of the FG microbeam (9) is rewritten in the following dimensionless form:

$$\bar{w}(0, \bar{t}) = \bar{w}(1, \bar{t}) = \frac{\partial \bar{w}(0, \bar{t})}{\partial \bar{x}} = \frac{\partial \bar{w}(1, \bar{t})}{\partial \bar{x}} = 0 \quad (15)$$

It can be seen that the equation of motion for the FG microbeam (11) is the nonlinear PDE which is very complicated. It is very difficult to find the exact solution of this equation. Therefore, the approximate method is an effective tool to find the approximate solution of the equation (11). In this work, the Galerkin method is used first to convert Eq. (11) into the ordinary differential equation (ODE). To apply the Galerkin method, the solution of Eq. (11) is assumed to have the following form:

$$\bar{w}(\bar{x}, \bar{t}) = Q(\bar{t}) \cdot \phi(\bar{x}), \quad (16)$$

where  $\phi(\bar{x})$  is the shape function to be chosen such that the solution (16) satisfies the kinematic boundary conditions (15) and  $Q(\bar{t})$  is a time-dependent function which needs to be found. Equation (16) implies that vibration of the FG microbeam is approximately one-mode vibration. Because the first mode is a basic and primary one of a like-beam structure. Furthermore, for micro-/nano-beams, approximate one-mode vibration shows accuracy [51, 52, 55, 58]. For the FG microbeam with two clamped ends, the shape function  $\phi(\bar{x})$  can be chosen as follows [55]:

$$\phi(\bar{x}) = \frac{1}{2} [1 - \cos(2\pi\bar{x})]. \quad (17)$$

Applying the Galerkin method for Eq. (11), one gets the nonlinear ODE as follows:

$$\ddot{Q} (c_1 + c_2 Q^2 + c_3 Q^4 + c_4 Q^6 + c_5 Q^8) + c_6 Q + c_7 Q^3 + c_8 Q^5 + c_9 Q^7 + c_{10} Q^9 + c_{11} Q^{11} = 0, \quad (18)$$

where,

$$c_1 = \bar{m}_0 \left( \int_0^1 \phi^2 d\bar{x} - \beta^2 \int_0^1 \phi \phi'' d\bar{x} \right), \quad (19)$$

$$c_2 = -4\bar{m}_0 \left( \int_0^1 \phi^4 d\bar{x} - \beta^2 \int_0^1 \phi^3 \phi'' d\bar{x} \right), \quad (20)$$

$$c_3 = 6\bar{m}_0 \left( \int_0^1 \phi^6 d\bar{x} - \beta^2 \int_0^1 \phi^5 \phi'' d\bar{x} \right), \quad (21)$$

$$c_4 = -4\bar{m}_0 \left( \int_0^1 \phi^8 d\bar{x} - \beta^2 \int_0^1 \phi^7 \phi'' d\bar{x} \right), \quad (22)$$

$$c_5 = \bar{m}_0 \left( \int_0^1 \phi^{10} d\bar{x} - \beta^2 \int_0^1 \phi^9 \phi'' d\bar{x} \right), \quad (23)$$

$$c_6 = \bar{D}_{xx} \left( \int_0^1 \phi \phi^{(4)} d\bar{x} - \alpha^2 \int_0^1 \phi \phi^{(6)} d\bar{x} \right) - \frac{V^2}{12} \int_0^1 \phi^2 d\bar{x} + \frac{V^2}{12} \beta^2 \int_0^1 \phi \phi'' d\bar{x} - H^2 \left( \int_0^1 \phi \phi'' d\bar{x} - \beta^2 \int_0^1 \phi \phi^{(4)} d\bar{x} \right), \quad (24)$$

$$c_7 = \left[ -\frac{\bar{A}_{xx}}{2} \delta^2 \int_0^1 (\phi')^2 d\bar{x} + \bar{A}_{xx} \delta^2 \alpha^2 \int_0^1 \phi' \phi''' d\bar{x} + \bar{A}_{xx} \delta^2 \alpha^2 \int_0^1 (\phi'')^2 d\bar{x} \right] \left( \int_0^1 \phi \phi'' d\bar{x} - \beta^2 \int_0^1 \phi \phi^{(4)} d\bar{x} \right) - 4\bar{D}_{xx} \left( \int_0^1 \phi^3 \phi^{(4)} d\bar{x} - \alpha^2 \int_0^1 \phi^3 \phi^{(6)} d\bar{x} \right) + \frac{V^2}{6} \int_0^1 \phi^4 d\bar{x} + V^2 \beta^2 \int_0^1 \phi^2 (\phi')^2 d\bar{x} + \frac{V^2}{6} \beta^2 \int_0^1 \phi^3 \phi'' d\bar{x} + 4H^2 \left( \int_0^1 \phi^3 \phi'' d\bar{x} - \beta^2 \int_0^1 \phi^3 \phi^{(4)} d\bar{x} \right), \quad (25)$$

$$c_8 = (-4) \left[ -\frac{\bar{A}_{xx}}{2} \delta^2 \int_0^1 (\phi')^2 d\bar{x} + \bar{A}_{xx} \delta^2 \alpha^2 \int_0^1 \phi' \phi''' d\bar{x} + \bar{A}_{xx} \delta^2 \alpha^2 \int_0^1 (\phi'')^2 d\bar{x} \right] \left( \int_0^1 \phi^3 \phi'' d\bar{x} - \beta^2 \int_0^1 \phi^3 \phi^{(4)} d\bar{x} \right) + 6\bar{D}_{xx} \left( \int_0^1 \phi^5 \phi^{(4)} d\bar{x} - \alpha^2 \int_0^1 \phi^5 \phi^{(6)} d\bar{x} \right) - \frac{V^2}{12} \int_0^1 \phi^6 d\bar{x} + V^2 \beta^2 \int_0^1 \phi^4 (\phi')^2 d\bar{x} - \frac{V^2}{4} \beta^2 \int_0^1 \phi^5 \phi'' d\bar{x} - 6H^2 \left( \int_0^1 \phi^5 \phi'' d\bar{x} - \beta^2 \int_0^1 \phi^5 \phi^{(4)} d\bar{x} \right), \quad (26)$$



$$c_9 = 6 \left[ -\frac{\bar{A}_{xx}}{2} \delta^2 \int_0^1 (\phi')^2 d\bar{x} + \bar{A}_{xx} \delta^2 \alpha^2 \int_0^1 \phi' \phi''' d\bar{x} + \bar{A}_{xx} \delta^2 \alpha^2 \int_0^1 (\phi'')^2 d\bar{x} \right] \left[ \int_0^1 \phi^5 \phi'' d\bar{x} - \beta^2 \int_0^1 \phi^5 \phi^{(4)} d\bar{x} \right] \\ - 4\bar{D}_{xx} \left( \int_0^1 \phi^7 \phi^{(4)} d\bar{x} - \alpha^2 \int_0^1 \phi^7 \phi^{(6)} d\bar{x} \right) + 4H^2 \left( \int_0^1 \phi^7 \phi'' d\bar{x} - \beta^2 \int_0^1 \phi^7 \phi^{(4)} d\bar{x} \right), \quad (27)$$

$$c_{10} = -4 \left[ -\frac{\bar{A}_{xx}}{2} \delta^2 \int_0^1 (\phi')^2 d\bar{x} + \bar{A}_{xx} \delta^2 \alpha^2 \int_0^1 \phi' \phi''' d\bar{x} + \bar{A}_{xx} \delta^2 \alpha^2 \int_0^1 (\phi'')^2 d\bar{x} \right] \left[ \int_0^1 \phi^7 \phi'' d\bar{x} - \beta^2 \int_0^1 \phi^7 \phi^{(4)} d\bar{x} \right] \\ + \bar{D}_{xx} \left( \int_0^1 \phi^9 \phi^{(4)} d\bar{x} - \alpha^2 \int_0^1 \phi^9 \phi^{(6)} d\bar{x} \right) - H^2 \left( \int_0^1 \phi^9 \phi'' d\bar{x} - \beta^2 \int_0^1 \phi^9 \phi^{(4)} d\bar{x} \right), \quad (28)$$

$$c_{11} = \left[ -\frac{\bar{A}_{xx}}{2} \delta^2 \int_0^1 (\phi')^2 d\bar{x} + \bar{A}_{xx} \delta^2 \alpha^2 \int_0^1 \phi' \phi''' d\bar{x} + \bar{A}_{xx} \delta^2 \alpha^2 \int_0^1 (\phi'')^2 d\bar{x} \right] \left[ \int_0^1 \phi^9 \phi'' d\bar{x} - \beta^2 \int_0^1 \phi^9 \phi^{(4)} d\bar{x} \right]. \quad (29)$$

Equation (18) is a nonlinear ODE which is assumed to satisfy the following initial conditions:

$$Q(0) = Q_0, \dot{Q}(0) = 0. \quad (30)$$

where  $Q_0 = \bar{w}_{\max}(0.5)$  is the maximum dimensionless initial amplitude of the FG microbeam.

### 3. Solution Procedure

With the help of the Galerkin method, the equation of motion for the FG microbeam is reduced to the nonlinear ODE (18). There are many analytical methods to find the approximate solution of Eq. (18) [60], in this section, the Hamiltonian Approach [61] will be applied to find the approximate solution of Eq. (18). The Hamiltonian Approach was proposed by He in 2010, this method is quite simple but effective in finding approximate analytical solution of ordinary differential equations [60, 61]. First, the Hamiltonian function of Eq. (18) is constructed as:

$$HF = \frac{1}{2} \dot{Q}^2 (c_1 + c_2 Q^2 + c_3 Q^4 + c_4 Q^6 + c_5 Q^8) + \frac{1}{2} c_6 Q^2 + \frac{1}{4} c_7 Q^4 + \frac{1}{6} c_8 Q^6 + \frac{1}{8} c_9 Q^8 + \frac{1}{10} c_{10} Q^{10} + \frac{1}{12} c_{11} Q^{12}. \quad (31)$$

Integrating Eq. (31) with respect to  $\bar{t}$  from 0 to  $T/4$ , leads to:

$$\overline{HF} = \int_0^{T/4} \left[ \frac{1}{2} \dot{Q}^2 (c_1 + c_2 Q^2 + c_3 Q^4 + c_4 Q^6 + c_5 Q^8) + \frac{1}{2} c_6 Q^2 + \frac{1}{4} c_7 Q^4 + \frac{1}{6} c_8 Q^6 + \frac{1}{8} c_9 Q^8 + \frac{1}{10} c_{10} Q^{10} + \frac{1}{12} c_{11} Q^{12} \right] d\bar{t}, \quad (32)$$

in which  $T$  is the period of the nonlinear vibration.

The approximate solution of Eq. (18) with the initial conditions (30) is assumed to have a following form:

$$Q(\bar{t}) = Q_0 \cos(\omega \bar{t}), \quad (33)$$

where  $\omega$  is the approximate nonlinear frequency of the FG microbeam.

Substituting Eq. (33) into Eq. (32), the expression of the Hamiltonian function can be obtained as:

$$\overline{HF} = \int_0^{T/4} \left[ \frac{1}{2} [-Q_0 \omega \sin(\omega \bar{t})]^2 [c_1 + c_2 Q_0^2 \cos^2(\omega \bar{t}) + c_3 Q_0^4 \cos^4(\omega \bar{t}) + c_4 Q_0^6 \cos^6(\omega \bar{t}) + c_5 Q_0^8 \cos^8(\omega \bar{t})] \right. \\ \left. + \frac{1}{2} c_6 Q_0^2 \cos^2(\omega \bar{t}) + \frac{1}{4} c_7 Q_0^4 \cos^4(\omega \bar{t}) + \frac{1}{6} c_8 Q_0^6 \cos^6(\omega \bar{t}) + \frac{1}{8} c_9 Q_0^8 \cos^8(\omega \bar{t}) + \frac{1}{10} c_{10} Q_0^{10} \cos^{10}(\omega \bar{t}) + \frac{1}{12} c_{11} Q_0^{12} \cos^{12}(\omega \bar{t}) \right] d\bar{t}. \quad (34)$$

Performing the integrals in Eq. (34), one gets the expression of the Hamiltonian function as follows:

$$\overline{HF} = \frac{1}{\omega} \left[ \left( \frac{1}{8} c_1 Q_0^2 + \frac{1}{32} c_2 Q_0^4 + \frac{1}{64} c_3 Q_0^6 + \frac{5}{512} c_4 Q_0^8 + \frac{7}{1024} c_5 Q_0^{10} \right) \pi \omega^2 + \right. \\ \left. \left( \frac{1}{8} c_6 Q_0^2 + \frac{3}{64} c_7 Q_0^4 + \frac{5}{192} c_8 Q_0^6 + \frac{35}{2048} c_9 Q_0^8 + \frac{63}{5120} c_{10} Q_0^{10} + \frac{77}{8192} c_{11} Q_0^{12} \right) \pi \right]. \quad (35)$$

The approximate frequency of the FG microbeam can be found by setting  $\partial(\partial \overline{HF} / \partial(1/\omega)) / \partial Q_0 = 0$ , as:

$$\omega_{NL} = \sqrt{\frac{c_6 + \frac{3}{4} c_7 Q_0^2 + \frac{5}{8} c_8 Q_0^4 + \frac{35}{64} c_9 Q_0^6 + \frac{63}{128} c_{10} Q_0^8 + \frac{231}{512} c_{11} Q_0^{10}}{c_1 + \frac{1}{2} c_2 Q_0^2 + \frac{3}{8} c_3 Q_0^4 + \frac{5}{16} c_4 Q_0^6 + \frac{35}{128} c_5 Q_0^8}}. \quad (36)$$

Finally, the approximate solution can be get by putting Eq. (36) into Eq. (33):

$$Q(\bar{t}) = Q_0 \cos \left[ \sqrt{\frac{c_6 + \frac{3}{4} c_7 Q_0^2 + \frac{5}{8} c_8 Q_0^4 + \frac{35}{64} c_9 Q_0^6 + \frac{63}{128} c_{10} Q_0^8 + \frac{231}{512} c_{11} Q_0^{10}}{c_1 + \frac{1}{2} c_2 Q_0^2 + \frac{3}{8} c_3 Q_0^4 + \frac{5}{16} c_4 Q_0^6 + \frac{35}{128} c_5 Q_0^8}} \bar{t} \right]. \quad (37)$$



**Table 1.** The material properties of Aluminum (Al) and Alumina ( $\text{Al}_2\text{O}_3$ )

Materials	Young's modulus $E$ (GPa)	Mass density $\rho$ ( $\text{kg/m}^3$ )
Aluminum (Al)	$E_m = 70$	$\rho_m = 2702$
Alumina ( $\text{Al}_2\text{O}_3$ )	$E_c = 380$	$\rho_c = 3960$

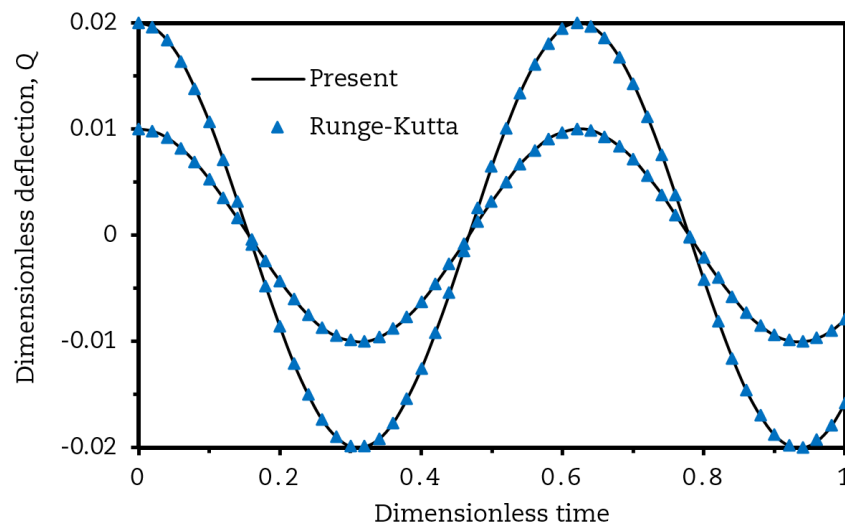
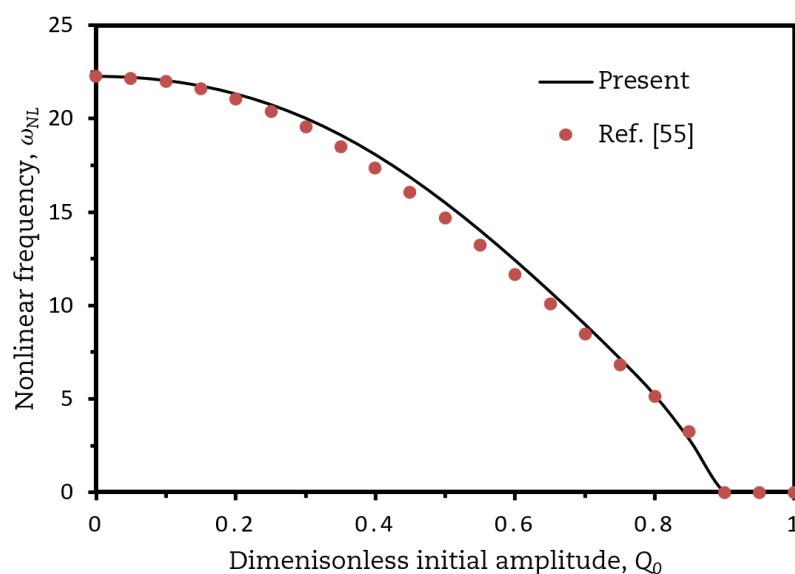
## 4. Numerical Results

In this section, numerical illustrations will be performed to evaluate the reliability of the research model as well as evaluate effects of the system parameters on the nonlinear vibration response of the FG microbeam. For this study, the FG microbeam made of Aluminum (Al - metal) and Alumina ( $\text{Al}_2\text{O}_3$  - ceramic) is considered. The material properties of the FG microbeam are shown in Table 1.

### 4.1 Comparison study

To verify the accuracy of the obtained solution, the analytical solution obtained in this work is compared with the numerical solution using the 4<sup>th</sup> order Runge-Kutta algorithm. The comparison results are shown in Fig. 2 for fixed values of  $k = 5$ ,  $\alpha = 0.01$ ,  $\beta = 0.01$ ,  $\delta = 3$ ,  $V = 5$  and  $H = 1$ . It can be observed from this figure that the obtained analytical solution has a very good accuracy compared to the numerical solution.

For the homogeneous microbeam, the frequencies obtained in this work and those obtained by Dang et al. [55] using the Equivalent Linearization method are also compared and shown in Fig. 3. The variation of the approximate nonlinear frequencies found by two analytical methods to the initial amplitude  $Q_0$  is presented in Fig. 3 for  $\alpha = 0.01$ ,  $\beta = 0.01$ ,  $L/h = 10$ ,  $g_0/L = 0.2$  and  $V = 5$ . The accuracy of the current approximate frequency and the approximate frequency achieved by Dang et al. [55] can be observed from this Figure.

**Fig. 2.** Comparison of the analytical solution with the numerical solution**Fig. 3.** The variation of the approximate nonlinear frequencies to the initial amplitude



**Table 3.** Comparison of the approximate frequencies of MEMS

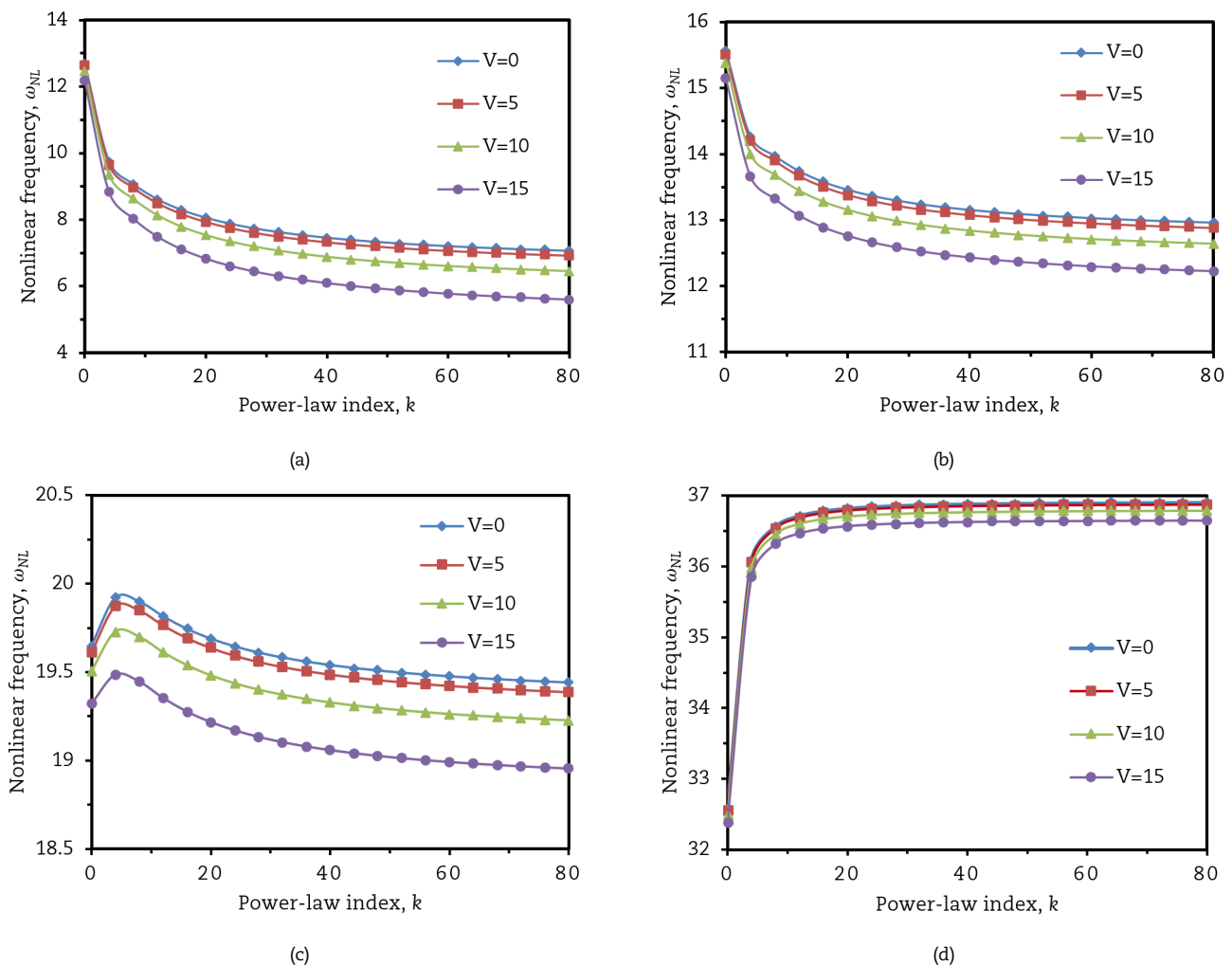
$Q_0$	$V$	$\omega_{EBM}$ [24]	$\omega_{Present}$
0.01	2	22.3628	22.3628
0.1		22.5680	22.5677
0.3		24.0554	24.0319
0.01	5	21.8882	21.8882
0.1		22.0943	22.0940
0.3		23.5839	23.5602

Based on the classical elasticity theory, the model studied in this work was investigated by Fu et al. [24] employing the Energy Balance method (EBM). For case of  $\delta = 24$  and some values of the initial amplitude  $Q_0$  and the applied voltage  $V$ , the approximate frequency obtained in this work and the one obtained by Fu et al. [24] are compared and presented in Table 2. Consistency between the approximate frequencies obtained by the two analytical methods can be observed from this Table.

In the below sub-sections, effects of the power-law index ( $k$ ), the material length scale parameter ( $\alpha$ ), the nonlocal parameter ( $\beta$ ), the applied voltage ( $V$ ) and the magnetic field ( $H$ ) on the nonlinear vibration behaviour of the FG microbeam are investigated and discussed.

#### 4.2 Effect of the power-law index

Effect of the power-law index  $k$  on the nonlinear vibration response of the FG microbeam is illustrated in Fig.4. This Figure is plotted with fixed values of the parameters as  $\alpha = 0.01$ ,  $\beta = 0.01$ ,  $\delta = 6$  and  $Q_0 = 0.01$ . Without the influence of the magnetic field ( $H = 0$ ), it can see from Fig.4a, the nonlinear frequency of the FG microbeam decreases as the power-law index  $k$  increases. This is appropriate because when the power-law index  $k$  increases, the volume fraction of metal constituent increases, this makes the FG microbeam more flexible (i.e. softer), and consequently the frequency of the FG microbeam decreases. The nonlinear frequency of the FG microbeam is larger than the one of the fully metal microbeam and smaller than the one of the fully ceramic microbeam. However, with the effect of the magnetic field, as can be observed from Fig. 4(b), (c) and (d), an increase in the power-law index  $k$  leads to an increase or a decrease in the nonlinear frequency of the FG microbeam depending on the magnitude of the surrounding magnetic field. In an environment with a weak magnetic field, the nonlinear frequency of the FG microbeam decreases when the power-law index  $k$  increases (see Fig. 4(b)).



**Fig. 4.** The variation of the nonlinear frequency to the power-law index for some values of the applied voltage: (a)  $H = 0$ , (b)  $H = 3$ , (c)  $H = 5$  and (d)  $H = 10$



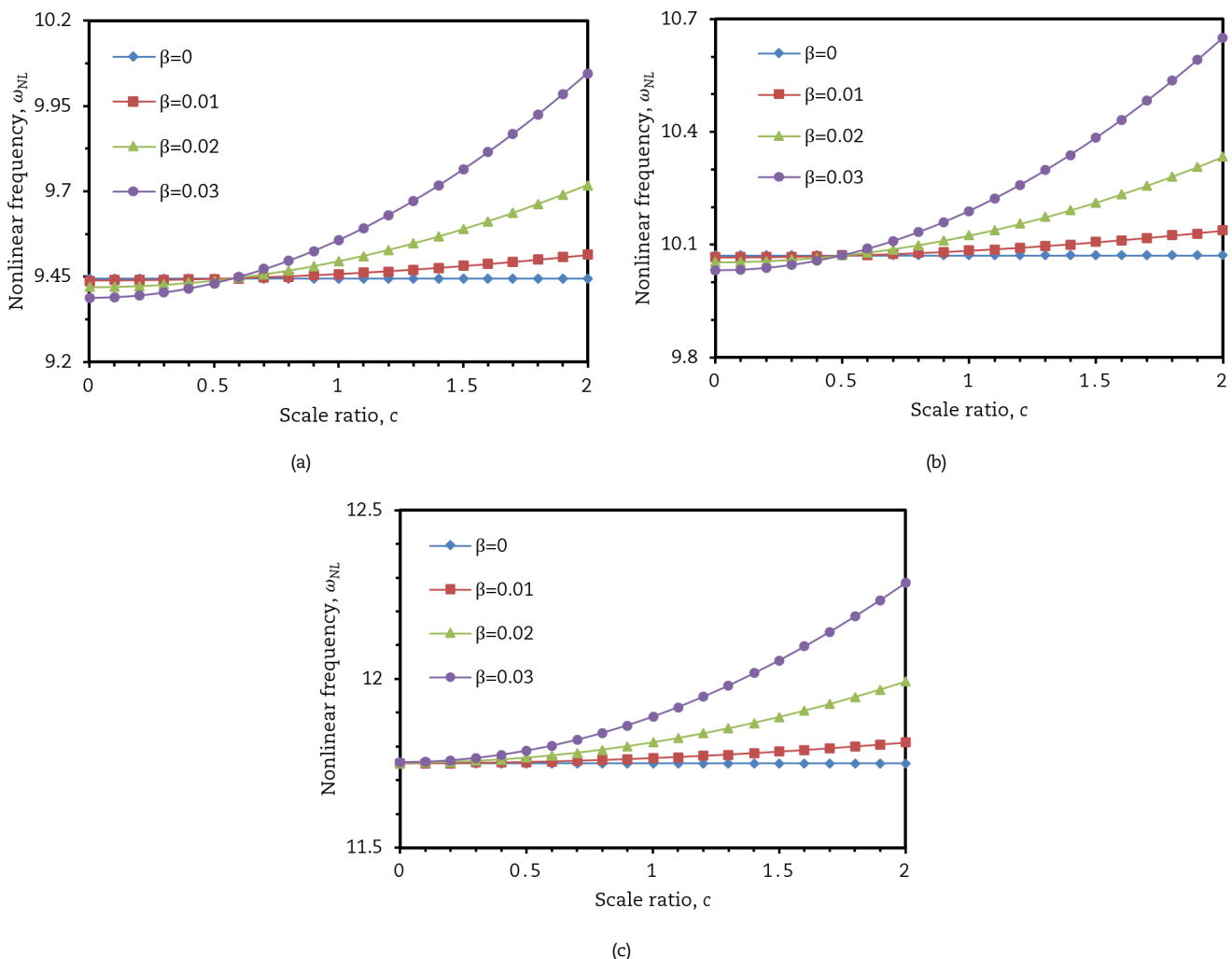
In an environment with a medium magnetic field, it can see from Fig. 4(c) that the nonlinear frequency of the FG microbeam increases for small values of the power-law index and decreases with larger values of the power-law index. With the selected values of the parameters to plot Fig. 4(c), the nonlinear frequency of the FG microbeam reaches to its maximum value when the power-law index  $k$  is about 5 ( $k \approx 5$ ). And in an environment with a strong magnetic field, the nonlinear frequency of the FG microbeam increases strongly when the power-law index increases specially for small values of the power-law index ( $k < 10$ ) (as can see from Fig. 4(d)); and for larger values of the power-law index, the nonlinear frequency of the FG microbeam do not change much as the power-law index varies. This can be explained because the magnetic field enhances the stiffness of the FG microbeam while the power-law index reduces the stiffness of the FG microbeam; therefore when the magnetic field is strong, the nonlinear frequency of the FG microbeam increases regardless the value of the power-law index  $k$ .

#### 4.3 Effects of the material length scale and nonlocal parameters

To study effect of the size-dependence on the vibration response of the FG microbeam, the scale ratio is defined as:

$$c = \frac{\alpha}{\beta} = \frac{l_m}{ea} \quad (38)$$

With fixed values of  $k=5$ ,  $\delta=6$ ,  $V=2$ , and  $Q_0=0.01$  Fig. 5 depicts the variation of the nonlinear frequency  $\omega_{NL}$  to the scale ratio  $c$  for some values of the nonlocal parameter  $\beta$ . It can be observed that the magnetic field has an important influence on the size-dependent vibration behaviour of the FG microbeam. From the published results based on the NSGT [55, 56, 58, 59], the FG microbeam exerts the softening effect or the hardening effect which depends on the relationship between the nonlocal parameter  $\beta$  and the material length scale parameter  $\alpha$ . However, it can be seen that under the influence of the magnetic field, the size-dependent vibration behaviour of the FG microbeam depends not only on the scale ratio  $c$  but also on the surrounding magnetic field ( $H$ ). Without the magnetic field, the FG microbeam exerts the hardening effect when the scale ratio  $c > 0.6$  (as can see from Fig. 5(a)). It means that the nonlinear frequencies of the nonlocal strain gradient FG microbeam are always larger than those of the classical FG microbeam when  $c > 0.6$  (i.e.,  $\alpha > 0.6\beta$ ) and the nonlinear frequencies of the nonlocal strain gradient FG microbeam are always smaller than those of the classical FG microbeam when  $c < 0.6$  (i.e.,  $\alpha < 0.6\beta$ ). When the magnetic field is small as can see from Fig. 5(b), the FG microbeam exerts the softening effect when the scale ratio  $c < 0.5$ . And in an environment with a strong magnetic field (as can see from Fig. 5(c)), the nonlinear frequencies of the nonlocal strain gradient FG microbeam are always larger than those of the classical FG microbeam for all values of the scale ratio.



**Fig. 5.** The variation of the nonlinear frequency to the scale ratio for some values of the nonlocal parameter: (a)  $H = 0$ , (b)  $H = 1$  and (c)  $H = 2$





#### 4.4 Effects of the applied voltage

Figures 6-8 depict the effect of the applied voltage  $V$  on the nonlinear vibration of the FG microbeam. Figure 6 is plotted with  $k=5$ ,  $\alpha=0.05$ ,  $\delta=6$ ,  $H=1$ ,  $Q_0=0.01$  and some values of the nonlocal parameter ( $\beta=0, 0.01, 0.05$  and  $0.1$ ). Figure 7 depicts the variation of the nonlinear frequency to the applied voltage for some values of the material length scale parameter and fixed values of  $k=10$ ,  $\beta=0.01$ ,  $\delta=6$ ,  $H=2$  and  $Q_0=0.01$ . And with chosen values of  $\alpha=0.01$ ,  $\beta=0.02$ ,  $\delta=6$ ,  $H=2$  and  $Q_0=0.01$ , Fig. 8 illustrates the variation of the nonlinear frequency to the applied voltage for some values of the power-law index ( $k=0, 0.5, 1, 2$  and  $5$ ). It can be seen from these Figures that the nonlinear frequency of the FG microbeam decreases when the applied voltage increases. For a fixed value of the applied voltage, the nonlinear frequency of the FG microbeam increases when the material length scale parameter  $\alpha$  increases. While for a fixed value of the applied voltage, the nonlinear frequency of the FG microbeam decreases or increases by increasing the nonlocal parameter and the power-law index depending on the magnitude of the magnetic field. From Fig. 6, it can be estimated that the nonlinear frequency of the FG microbeam decreases about 5% when the dimensionless applied voltage  $V$  increases from 5 to 10.

In the stability configuration, the applied voltage leads to a decrease of the frequency of the FG microbeam; but when the applied voltage exceeds the critical voltage  $V_{cr}$ , the frequency of the FG microbeam will fall to zero and the instability phenomena occurs. It can be observed from Figs. 6-8 that the material length scale parameter leads to an increase of the critical voltage  $V_{cr}$ ; on the other hand, the nonlocal parameter and the power-law index lead to a decrease or an increase of the critical voltage  $V_{cr}$  depending on the magnitude of the magnetic field. Analysis of instability of the FG microbeam under the electrostatic force is an interesting problem and needs to be studied in more details.

#### 4.5 Effects of the magnetic field

In this sub-section, effect of the magnetic field on the nonlinear frequency of the FG microbeam is also investigated and presented in Figs. 9 to 12. Figure 9 presents the variation of the nonlinear frequency to the magnetic field for some values of the power-law index  $k$  and selected values of  $\alpha=0.01$ ,  $\beta=0.01$ ,  $\delta=6$ ,  $V=2$  and  $Q_0=0.01$ . The variation of the nonlinear frequency to the magnetic field is shown in Fig. 10 for some values of the nonlocal parameter and specific values of  $k=5$ ,  $\alpha=0.01$ ,  $\delta=6$ ,  $V=2$  and  $Q_0=0.01$ . With fixed values of  $k=5$ ,  $\beta=0.01$ ,  $\delta=6$ ,  $V=2$  and  $Q_0=0.01$ ; Fig. 11 depicts the variation of the nonlinear frequency to the magnetic field for some values of material length scale parameter ( $\alpha=0, 0.05, 0.1$  and  $0.15$ ). And the variation of the nonlinear frequency to the magnetic field for various values of the applied voltage is presented in Fig. 12 with selected values of  $k=5$ ,  $\alpha=0.01$ ,  $\beta=0.01$ ,  $\delta=6$  and  $Q_0=0.01$ . It can be concluded that the magnetic field leads to an increase in the nonlinear frequency of the FG microbeam.

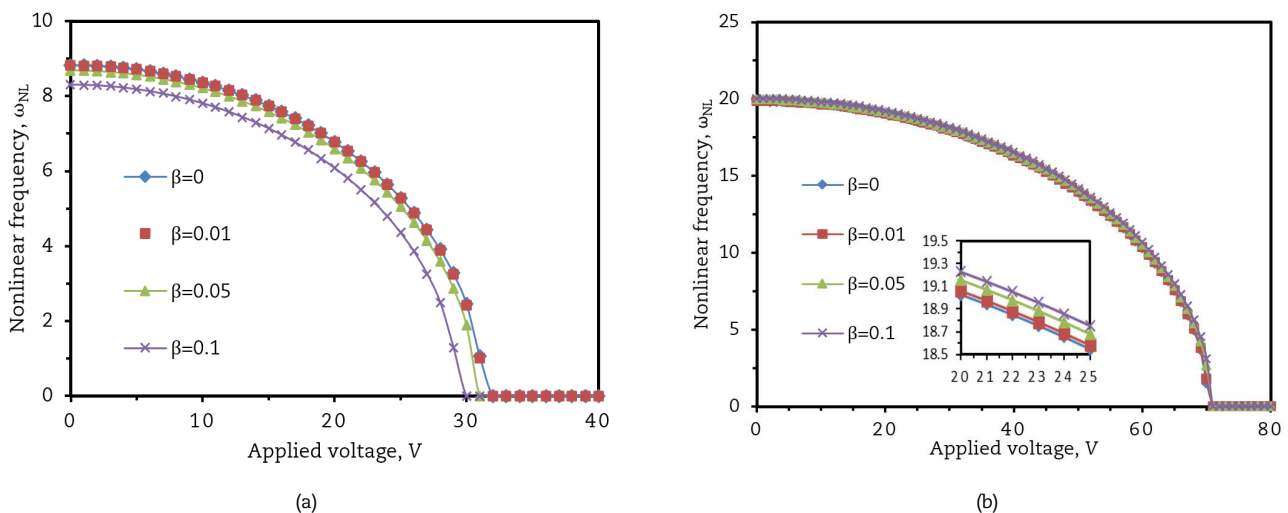


Fig. 6. The variation of the nonlinear frequency to the applied voltage for some values of the nonlocal parameter: (a)  $H=0$  and (b)  $H=5$

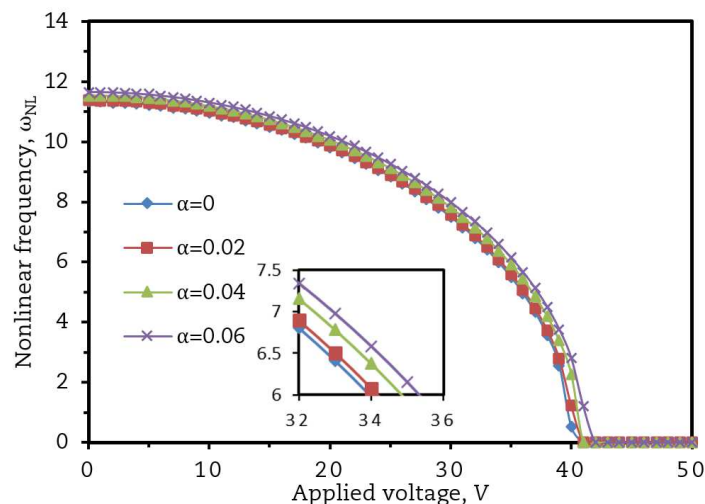
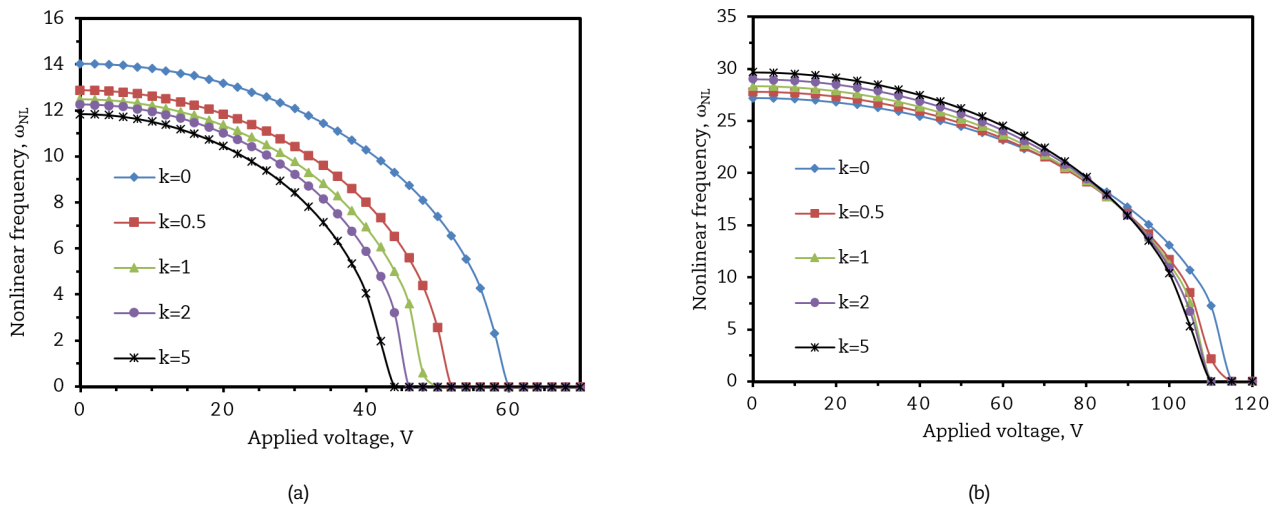
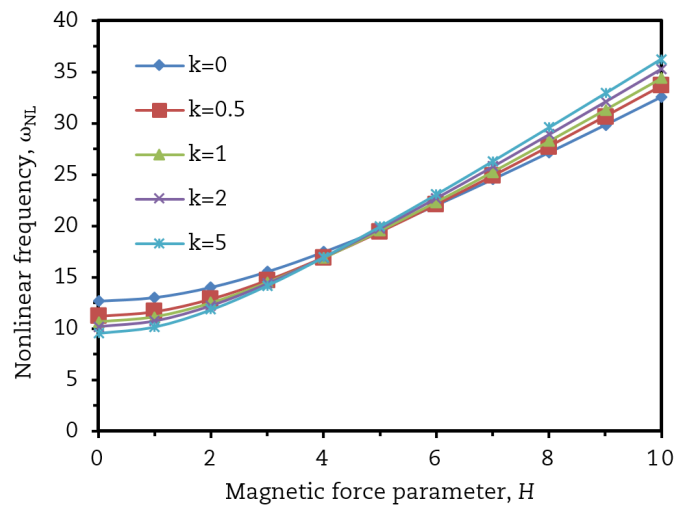


Fig. 7. The variation of the nonlinear frequency to the applied voltage for some values of the material length scale parameter:  $H=2$

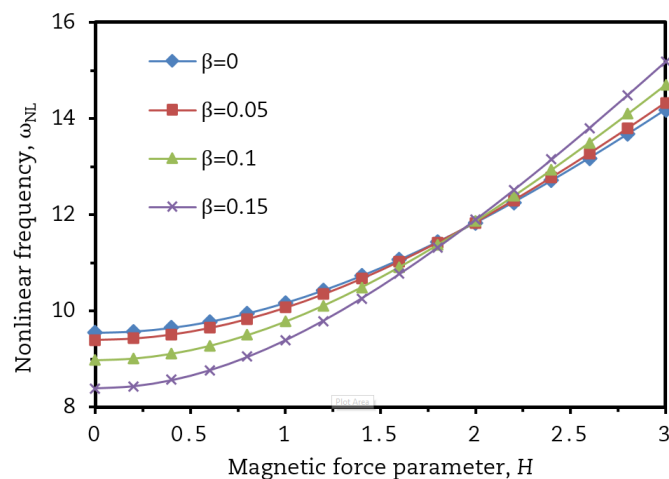




**Fig. 8.** The variation of the nonlinear frequency to the applied voltage for some values of the power-law index; ((a)  $H = 2$  and (b)  $H = 8$ )



**Fig. 9.** The variation of the nonlinear frequency to the magnetic force parameter for some values of the power-law index



**Fig. 10.** The variation of the nonlinear frequency to the magnetic force parameter for some values of the nonlocal parameter

This observation is completely consistent with the results obtained by Ebrahimi and Barati [57]. And for a fixed value of the magnetic force parameter  $H$ , the nonlinear frequency of the FG microbeam increases by increasing the material length scale parameter  $\alpha$  or by reducing the applied voltage  $V$  (see Figs. 11 and 12). And on the other hand, Figs. 9 and 10 reveal that the nonlinear frequency of the FG microbeam increases or decreases by increasing the power-law index  $k$  and the nonlocal parameter  $\beta$  which depends on the magnitude of the magnetic field. For small values of the magnetic force parameter  $H$ , the nonlinear frequency of the FG microbeam decreases when the power-law index  $k$  and the nonlocal parameter  $\beta$  increase; while for large values of the magnetic force parameter  $H$ , the nonlinear frequency of the FG microbeam increases when the power-law index  $k$  and the nonlocal parameter  $\beta$  increase.



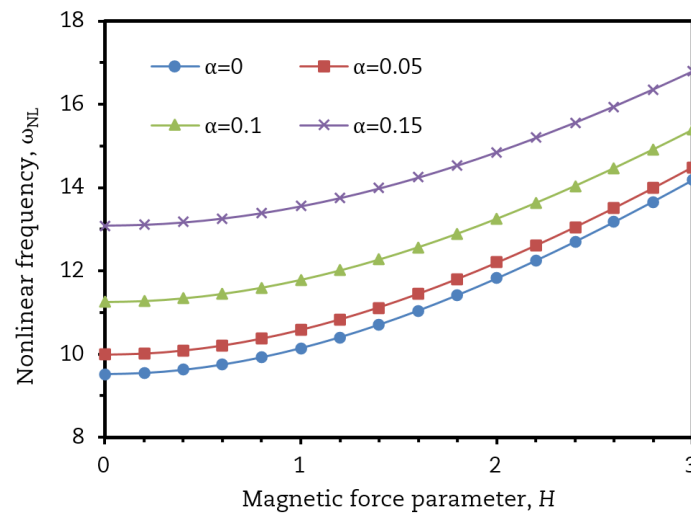


Fig. 11. The variation of the nonlinear frequency to the magnetic force parameter for some values of the material length scale parameter

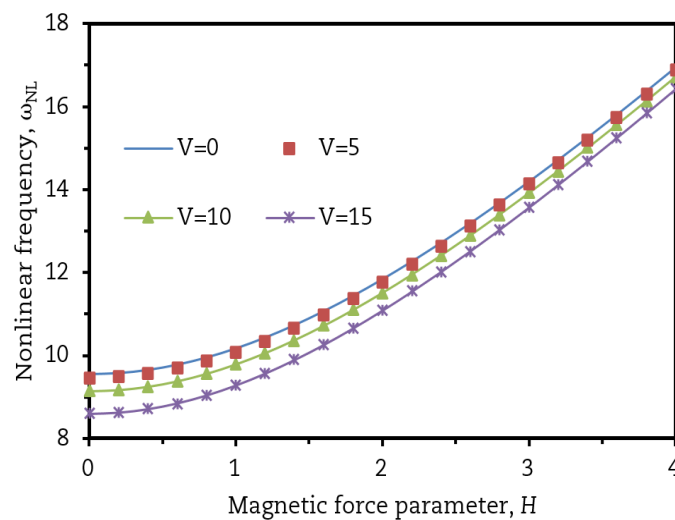


Fig. 12. The variation of the nonlinear frequency to the magnetic force parameter for some values of the applied voltage

## 5. Conclusion

A model of an electrostatically actuated FG microbeam under a longitudinal magnetic field is developed for the first time in this work by using the EBT and the NSGT to investigate the nonlinear vibration problem. A DC voltage applied between the two fixed electrodes causes the electrostatic force to be exerted on the FG microbeam which is placed between the two fixed electrodes. Besides the electrostatic force, the effect of the longitudinal magnetic field is also considered in this model. The analytical expression of the approximate nonlinear frequency of the FG microbeam was obtained by utilizing the Galerkin method and the Hamiltonian Approach. Numerical illustrations were performed to verify the accuracy of the research model as well as to examine effects of the parameters on the nonlinear vibration behaviour of the FG microbeam. Some of important conclusions can be summarized as follows:

- When the power-law index  $k$  increases, the nonlinear frequency  $\omega_{NL}$  of the FG microbeam decreases or increases depending on the magnitude of the magnetic field.
- The nonlinear frequency  $\omega_{NL}$  of the FG microbeam decreases by increasing the nonlocal parameter  $\beta$  and by reducing the material length scale parameter  $\alpha$ . The FG microbeam exerts the softening-effect and hardening-effect which depends not only on the scale parameters but also on the magnetic field.
- The applied voltage  $V$  leads to a reduce of the nonlinear frequency  $\omega_{NL}$  of the FG microbeam. However, the FG microbeam will be unstable if the applied voltage  $V$  exceeds its critical value.
- The magnetic field  $H$  has an important influence on the vibration behaviour of the FG microbeam, the magnetic field  $H$  leads to an increase in the nonlinear frequency  $\omega_{NL}$  of the FG microbeam regardless of the values of power-law index  $k$  and the nonlocal parameter  $\beta$ .

## Author Contributions

Dang Van Hieu planned the scheme, initiated the project, and suggested the mathematical model; Nguyen Thi Hoa solved the proposed mathematical model; Le Quang Duy examined the theory validation; Nguyen Thi Kim Thoa checked the formulation and the obtained results. The manuscript was written through the contribution of all authors. All authors discussed the results, reviewed, and approved the final version of the manuscript.



## Acknowledgments

This work is supported by TNU, Thai Nguyen University of Technology (TNUT) under grant number “ĐH2019-TN02-03”.

## Conflict of Interest

The authors declared no potential conflicts of interest with respect to the research, authorship, and publication of this article.




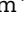
## References

- [1] Batra, R.C., Porfiri, M., Spinello, D., Review of modeling electrostatically actuated microelectromechanical systems, *Smart Materials and Structures*, 16, 2007, 23–31.
- [2] Dean, R. N., Luque, A., Applications of microelectromechanical systems in industrial processes and services, *IEEE Transactions on Industrial Electronics*, 56, 2009, 913–925.
- [3] Zhang, W. M., Yan, H., Peng, Z. K., Meng, G., Electrostatic pull-in instability in MEMS/NEMS: A review, *Sensors and Actuators A*, 214, 2014, 187–218.
- [4] Batra, R. C., Porfiri, M., Spinello, D., Vibrations of narrow microbeams predeformed by an electric field, *Journal of Sound and Vibration*, 309(3–5), 2008, 600–612.
- [5] Rahman, E. M. A., Younis, M. I. and Nayfeh, A. H., Characterization of the mechanical behavior of an electrically actuated microbeam, *Journal of Micromechanics and Microengineering*, 12, 2002, 759–766.
- [6] Zand, M. M., Ahmadian, M.T., Rashidian, B., Semi-analytic solutions to nonlinear vibrations of microbeams under suddenly applied voltages, *Journal of Sound and Vibration*, 325(1–2), 2009, 382–396.
- [7] De, S. K. and Aluru, N. R., Complex Nonlinear Oscillations in Electrostatically Actuated Microstructures, *Journal of Microelectromechanical Systems*, 15(2), 2006, 355–369.
- [8] Krylov, S., Lyapunov exponents as a criterion for the dynamic pull-in instability of electrostatically actuated microstructures, *International Journal of Non-Linear Mechanics*, 42(4), 2007, 626–642.
- [9] Krylov, S., Dick, N., Dynamic stability of electrostatically actuated initially curved shallow micro beams, *Continuum Mechanics and Thermodynamics*, 22, 2010, 445–468.
- [10] Ruzziconi, L., Bataineh, A. M., Younis, M. I., Cui, W. and Lenci, S., Nonlinear dynamics of an electrically actuated imperfect microbeam resonator: experimental investigation and reduced-order modeling, *Journal of Micromechanics and Microengineering*, 23, 2013, 075012.
- [11] Askari, A. R., Tahani, M., Stability analysis of electrostatically actuated nano/micro-beams under the effect of van der Waals force, a semi-analytical approach, *Communications in Nonlinear Science and Numerical Simulation*, 34, 2016, 130–141.
- [12] Harsha, S.C., Prasanth, C.S. and Pratiher, B., Prediction of pull-in phenomena and structural stability analysis of an electrostatically actuated microswitch, *Acta Mechanica*, 227, 2016, 2577–2594.
- [13] Bhojwala, V.M., Vakharia, D.P., Closed-form relation to predict static pull-in voltage of an electrostatically actuated clamped–clamped microbeam under the effect of Casimir force, *Acta Mechanica*, 228, 2017, 2583–2602.
- [14] Ouakad, H.M., Nonlinear structural behavior of a size-dependent MEMS gyroscope assuming a non-trivial shaped proof mass, *Microsystem Technologies*, 26, 2020, 573–582.
- [15] Ouakad, H.M., Electrostatic fringing-fields effects on the structural behavior of MEMS shallow arches, *Microsystem Technologies*, 24, 2018, 1391–1399.
- [16] Tausiff, M., Ouakad, H.M., Alqahtani, H. et al., Local nonlinear dynamics of MEMS arches actuated by fringing-field electrostatic actuation, *Nonlinear Dynamics*, 95, 2019, 2907–2921.
- [17] Tausiff, M., Ouakad, H.M. & Alqahtani, H., Global Nonlinear Dynamics of MEMS Arches Actuated by Fringing-Field Electrostatic Field, *Arabian Journal for Science and Engineering*, 45, 2020, 5959–5975.
- [18] Ouakad, M., Sedighi, H.M., Static response and free vibration of MEMS arches assuming out-of-plane actuation pattern, *International Journal of Non-Linear Mechanics*, 110, 2019, 44–57.
- [19] Jabbari, G., Shabani, R. and Rezazadeh, G., Frequency response of an electrostatically actuated micro resonator in contact with incompressible fluid, *Microsystem Technologies*, 23, 2017, 2381–2391.
- [20] Ouakad, H.M., Ilyas, S., Younis, M.I. Investigating Mode Localization at Lower- and Higher-Order Modes in Mechanically Coupled MEMS Resonators, *Journal of Computational and Nonlinear Dynamics*, 15(3), 2020, 031001.
- [21] Alcheikh, N., Ouakad, H.M., Younis, M.I., Dynamics of V-Shaped Electrothermal MEMS-Based Resonators, *Journal of Microelectromechanical Systems*, 29(5), 2020, 1372–1381.
- [22] Hasan, M.H., Alsaleem, F.M., Ouakad, H.M., Novel threshold pressure sensors based on nonlinear dynamics of MEMS resonators, *Journal of Micromechanics and Microengineering*, 28(6), 2018, 065007.
- [23] Ouakad, H.M., Ilyas, S., Younis, M.I., Investigating Mode Localization at Lower- and Higher-Order Modes in Mechanically Coupled MEMS Resonators, *Journal of Computational and Nonlinear Dynamics*, 15(3), (2020), 031001.
- [24] Fu, Y. M., Zhang, J., Wan, L. J., Application of the energy balance method to a nonlinear oscillator arising in the microelectromechanical system (MEMS), *Current Applied Physics*, 11, 2011, 482–485.
- [25] Qian, Y. H., Ren, D. X., Lai, S. K., Chen, S. M., Analytical approximations to nonlinear vibration of an electrostatically actuated microbeam, *Communications in Nonlinear Science and Numerical Simulation*, 17, 2012, 1947–1955.
- [26] Hieu, D. V., Thoa, N. T. K., Duy, L. Q., Analysis of nonlinear oscillator arising in the microelectromechanical system by using the parameter expansion and equivalent linearization methods, *International Journal of Engineering & Technology*, 7(2), 2018, 597–604.
- [27] Chakraverty, S., Pradhan, K.K., *Vibration of Functionally Graded Beams and Plates*, Academic Press, 2016.
- [28] Thai, H.T., Vo, T.P., Bending and free vibration of functionally graded beams using various higher-order shear deformation beam theories, *International Journal of Mechanical Sciences*, 62(1), 2012, 57–66.
- [29] Kadoli, R., Akhtar, K., Ganesan, N., Static analysis of functionally graded beams using higher order shear deformation theory, *Applied Mathematical Modelling*, 32(12), 2008, 2509–2255.
- [30] Li, X.F., Wang, B.L., Han, J.C., A higher-order theory for static and dynamic analyses of functionally graded beams, *Archive of Applied Mechanics*, 80(10), 2010, 1197–1212.
- [31] Simsek, M., Fundamental frequency analysis of functionally graded beams by using different higher-order beam theories, *Nuclear Engineering and Design*, 240(4), 2010, 697–705.
- [32] Trinh, L.C., Nguyen, H.X., Vo, T.P., Nguyen, T.K., Size-dependent behaviour of functionally graded microbeams using various shear deformation theories based on the modified couple stress theory, *Composite Structures*, 154, 2016, 556–572.
- [33] Houari, M.S.A., Tounsi, A., Bessaim, A., Mahmoud, S. R., A new simple three-unknown sinusoidal shear deformation theory for functionally graded plates, *Steel and Composite Structures*, 22(2), 2016, 257–276.
- [34] Boudarba, B., Houari, M.S.A., Tounsi, A., Mahmoud, S. R., Thermal stability of functionally graded sandwich plates using a simple shear deformation theory, *Structural Engineering and Mechanics*, 58(3), 2016, 397–422.
- [35] Belabed, Z., Houari, M.S.A., Tounsi, A., Mahmoud, S.R., Bég, O.A., An efficient and simple higher order shear and normal deformation theory for functionally graded material (FGM) plates, *Composites: Part B*, 60, 2014, 274–283.
- [36] Bousahla, A.A., Benyoucef, S., Tounsi, A., Mahmoud, S.R., On thermal stability of plates with functionally graded coefficient of thermal expansion, *Structural Engineering And Mechanics*, 60(2), 2016, 313–335.
- [37] Bennoun, M., Houari, M.S.A., Tounsi, A., A novel five variable refined plate theory for vibration analysis of functionally graded sandwich plates, *Mechanics of Advanced Materials and Structures*, 23(4), 2016, 423–431.
- [38] Hebalı, H., Tounsi, A., Houari, M.S.A., Bessaim, A., A new quasi-3D hyperbolic shear deformation theory for the static and free vibration analysis of functionally graded plates, *ASCE Journal of Engineering Mechanics*, 140, 2014, 374–383.
- [39] Abualnour, M., Houari, M.S.A., Tounsi, Bedia, A.A., Mahmoud, S.R., A novel quasi-3D trigonometric plate theory for free vibration analysis of advanced composite plates, *Composite Structures*, 184, 2018, 688–697.



- [40] Eringen, A.C., Edelen, D.G.B., On nonlocal elasticity, *International Journal of Engineering Science*, 10, 1972, 233-48.
- [41] Eringen, A.C., On differential equations of nonlocal elasticity and solutions of screw dislocation and surface waves, *Journal of Applied Physics*, 54, 1983, 4703-4710.
- [42] Mindlin, R.D., Second gradient of strain and surface-tension in linear elasticity, *International Journal of Solids and Structures*, 1(1), 1965, 417-438.
- [43] Aifantis, E.C., On the role of gradients in the localization of deformation and fracture, *International Journal of Engineering Science*, 30(10), 1992, 1279-1299.
- [44] Lam, D.C.C., Yang, F., Chong, A.C.M., Wang, J., Tong, P., Experiments and theory in strain gradient elasticity, *Journal of Mechanics and Physics of Solids*, 51(8), 2003, 1477-1508.
- [45] Yang, F., Chong, A.C.M., Lam, D.C.C., Tong, P., Couple stress based strain gradient theory for elasticity, *International Journal of Solids and Structures*, 39(10), 2002, 2731-2743.
- [46] Lim, C.W., Zhang, G., Reddy, J.N., A higher-order nonlocal elasticity and strain gradient theory and its applications in wave propagation, *Journal of Mechanics and Physics of Solids*, 78, 2015, 298-313.
- [47] Kivi, A.R., Azizi, S., Norouzi, P., Bifurcation Analysis of an Electrostatically Actuated Nano-Beam Based on Modified Couple Stress Theory, *Sensing and Imaging*, 18(32), 2017.
- [48] Kong, S., Size effect on pull-in behavior of electrostatically actuated microbeams based on a modified couple stress theory, *Applied Mathematical Modelling*, 37, 2013, 7481-7488.
- [49] Beni, Y.T., Koochi, A., Abadyan, M., Theoretical study of the effect of Casimir force, elastic boundary conditions and size dependency on the pull-in instability of beam-type NEMS, *Physica E: Low-dimensional Systems and Nanostructures*, 43(4), 2011, 979-988.
- [50] Rokni, H., Seethaler, R.J., Milani, A.S., Hashemi, S.H., Li, X. F., Analytical closed-form solutions for size-dependent static pull-in behavior in electrostatic micro-actuators via Fredholm integral equation, *Sensors and Actuators A: Physical*, 190, 2013, 32-43.
- [51] Sedighi, H.M., Size-dependent dynamic pull-in instability of vibrating electrically actuated microbeams based on the strain gradient elasticity theory, *Acta Astronautica*, 95, 2014, 111-123.
- [52] Sedighi, H.M., The influence of small scale on the pull-in behavior of nonlocal nanobridges considering surface effect, Casimir and Van der Waals attractions, *International Journal of Applied Mechanics*, 06(03), 2014, 1450030.
- [53] Ataei, H., Tadi Beni, Y., Size-Dependent Pull-In Instability of Electrically Actuated Functionally Graded Nano-Beams Under Intermolecular Forces, *Iranian Journal of Science and Technology, Transactions of Mechanical Engineering*, 40, 2016, 289-301.
- [54] Shishesaz, M., Shirbani, M. M., Sedighi, H. M., Hajnayeb, A., Design and analytical modeling of magneto-electro-mechanical characteristics of a novel magneto-electro-elastic vibration-based energy harvesting system, *Journal of Sound and Vibration*, 425, 2018, 149-169.
- [55] Dang, V. H., Nguyen, D. A., Le, M. Q., Duong, T.H., Nonlinear vibration of nanobeams under electrostatic force based on the nonlocal strain gradient theory, *International Journal of Mechanics and Materials in Design*, 16, 2020, 289-308.
- [56] Esfahani, S., Khadem, S.E., Mamaghani, A.E., Nonlinear Vibration Analysis of an Electrostatic Functionally Graded Nano-Resonator with Surface Effects Based on Nonlocal Strain Gradient Theory, *International Journal of Mechanical Sciences*, 151, 2019, 508-522.
- [57] Ebrahimi, F. and Barati, M. R., Free vibration analysis of couple stress rotating nanobeams with surface effect under in-plane axial magnetic field, *Journal of Vibration and Control*, 24(21), 2017, 5097-5107.
- [58] Simsek, M., Nonlinear free vibration of a functionally graded nanobeam using nonlocal strain gradient theory and a novel Hamiltonian approach, *International Journal of Engineering Science*, 105, 2016, 12-27.
- [59] Li, L., Li, X., Hu, Y., Free vibration analysis of nonlocal strain gradient beams made of functionally graded material, *International Journal of Engineering Science*, 102, 2016, 77-92.
- [60] Bayat, M., Pakar, I. and Domairry, G., Recent developments of some asymptotic methods and their applications for nonlinear vibration equations in engineering problems: A review, *Latin American Journal of Solids and Structures*, 9, 2012, 145 - 234.
- [61] He, J. H., Hamiltonian approach to nonlinear oscillators, *Physics Letters A*, 374(23), 2010, 2312-2314.

## ORCID iD

Dang Van Hieu  <https://orcid.org/0000-0001-8789-7284>  
 Nguyen Thi Hoa  <https://orcid.org/0000-0003-3658-5998>  
 Le Quang Duy  <https://orcid.org/0000-0001-5013-7150>  
 Nguyen Thi Kim Thoa  <https://orcid.org/0000-0003-4876-8169>



© 2021 Shahid Chamran University of Ahvaz, Ahvaz, Iran. This article is an open access article distributed under the terms and conditions of the Creative Commons Attribution-NonCommercial 4.0 International (CC BY-NC 4.0 license) (<http://creativecommons.org/licenses/by-nc/4.0/>).

How to cite this article: Dang Van Hieu et al.. Nonlinear vibration of an electrostatically actuated functionally graded microbeam under longitudinal magnetic field, *J. Appl. Comput. Mech.*, 7(3), 2021, 1537-1549.  
<https://doi.org/10.22055/JACM.2021.35504.2670>

**Publisher's Note** Shahid Chamran University of Ahvaz remains neutral with regard to jurisdictional claims in published maps and institutional affiliations.

